Food & Function

Accepted Manuscript

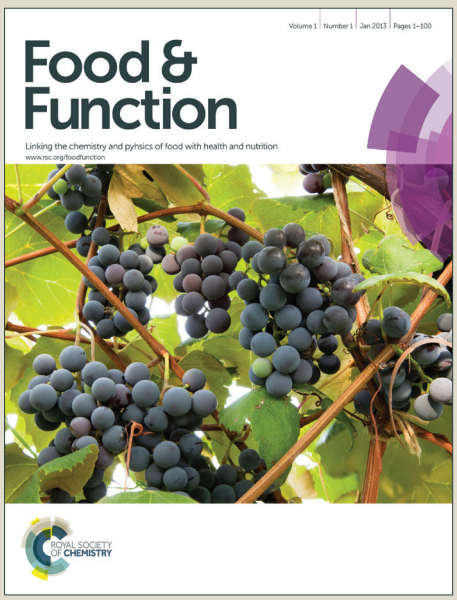

This is an *Accepted Manuscript*, which has been through the Royal Society of Chemistry peer review process and has been accepted for publication.

Accepted Manuscripts are published online shortly after acceptance, before technical editing, formatting and proof reading. Using this free service, authors can make their results available to the community, in citable form, before we publish the edited article. We will replace this *Accepted Manuscript* with the edited and formatted *Advance Article* as soon as it is available.

You can find more information about *Accepted Manuscripts* in the Information for Authors.

Please note that technical editing may introduce minor changes to the text and/or graphics, which may alter content. The journal's standard Terms & Conditions and the Ethical guidelines still apply. In no event shall the Royal Society of Chemistry be held responsible for any errors or omissions in this *Accepted Manuscript* or any consequences arising from the use of any information it contains.

ROYAL SOCIETY OF CHEMISTRY

www.rsc.org/foodfunction

Pomegranate phenolics inhibit formation of advanced glycation endproducts by scavenging reactive carbonyl species

Weixi Liu [1a], Hang Ma [2a], Leslie Frost [3], Tao Yuan [2, 4],

Joel A. Dain[1*], Navindra P. Seeram [2*]

[1] *Department of Chemistry, University of Rhode Island, Kingston, RI, 02881, USA*

[2] *Bioactive Botanical Research Laboratory, Department of Biomedical and Pharmaceutical Sciences, University of Rhode Island, Kingston, RI, 02881, USA*

[3] *Department of Chemistry, Marshall University, Huntington, WV, 25755, USA*

[4] *Xinjiang Technical Institute of Physics and Chemistry, Chinese Academy of Sciences, Urumqi 830011, China*

[a] These authors contributed equally to this work

* Corresponding authors:

***Joel A. Dain**
51 Lower College Road
Kingston, RI, United States
Fax: + (1) 401 874 5072
Phone: + (1) 401 874 5942
Email: jdain@chm.uri.edu

***Navindra P. Seeram**
7 Greenhouse Road
Kingston, RI, United States
Fax: + (1) 401 874 5787
Phone: + (1) 401 874 9367
Email: nseeram@uri.edu

The present study reported for the first time the inhibitory effects of pomegranate phenolics on the formation of advanced glycation endproducts and their carbonyl scavenger reactivity.

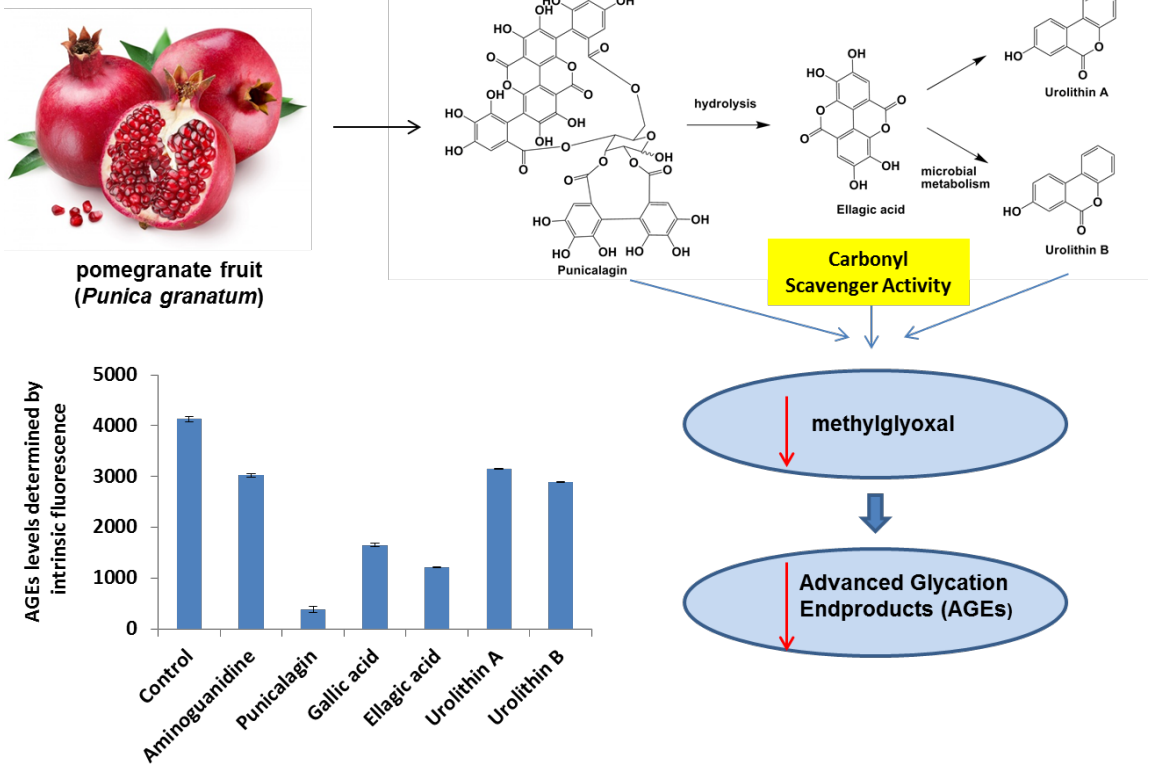

ABSTRACT

Advanced Glycation Endproducts (AGEs) are a heterogeneous group of molecules produced from non-enzymatic glycation. Accumulation of AGEs *in vivo* plays an important role in the pathology of chronic human diseases including type-2 diabetes and Alzheimer's disease. Natural AGEs inhibitors such as the pomegranate (*Punica granatum*) fruit show great potential for the management of these diseases. Herein, we investigated the *in vitro* anti-glycation effects of a pomegranate fruit extract (PE), its phenolic constituents [punicalagin (PA), ellagic acid (EA) and gallic acid (GA)], and their *in vivo* derived colonic metabolites [urolithin A (UA) and urolithin B (UB)]. All of the samples showed anti-glycation activities and PE, PA, and EA were more potent inhibitors than the positive control, aminoguanidine. PE and the purified phenolics also exhibited carbonyl scavenger reactivity. Our study suggests that pomegranate may offer an attractive dietary strategy for the prevention and treatment of AGE-related diseases such as type-2 diabetes and Alzheimer's disease.

Keywords: Glycation; AGEs; Pomegranate; *Punica granatum*; Phenolics; Urolithins

Abbreviations:

AGEs, Advanced Glycation Endproducts; PE, Pomegranate Extract; PA, Punicalagin; EA, Ellagic Acid; GA, Gallic Acid; UA, Urolithin A; UB, Urolithin B; MGO, Methylglyoxal; AG, Aminoguanidine; AD, Alzheimer's Disease; ROS, Reactive Oxygen Species; RCS, Reactive Carbonyl Species; Gly, Glyoxal; 3-DG, 3-Deoxyglucosone; BSA, Bovine Serum Albumin; PD, 1,2-Phenylenediamine; DQ, 2,3-Dimethylquinoxaline; TFA, Trifluoroacetic Acid; CD, Circular Dichroism; 2-MQ, 2-Methylquinoxaline

1. Introduction

The non-enzymatic reaction of reducing sugars with amino containing molecules such as proteins, peptides, or nucleic acids is referred to as glycation. Glycation occurs slowly *in vivo* and leads to the formation of a polymorphic group of compounds known as advanced glycation endproducts (AGEs) [1, 2]. The gradual build-up of AGEs in body tissues has been implicated as a major contributor to many progressive diseases including diabetic complications [3, 4] and Alzheimer's disease (AD) [5, 6]. AGEs play a role in the pathogenesis of such health disorders through two major mechanisms: 1) AGE modified plasma proteins could bind to AGE receptors (RAGE) on the surface of the cell, activate cell signaling and lead to the production of reactive oxygen species (ROS) and inflammatory factors [7] and, 2) proteins on the extracellular matrix crosslink with other matrix components, leading to the loss in their function [8]. Notably, increasing research has shown that AD pathogenesis is related to AGEs and AGE formation is accelerated in patients with AD [9]. AGE modified proteins can interact with neuron cell surface receptors such as RAGE and trigger oxidative stress and inflammation, subsequently leading to neuronal dysfunction [10]. The accumulation of AGEs is also responsible for protein-Aβ crosslinks, a major cause of neurodegeneration in AD [11].

Apart from reducing sugars, AGEs are also derived from reactive carbonyl species (RCS). Intracellular hyperglycemia induces the formation of glucose-derived RCS such as glyoxal (Gly), methylglyoxal (MGO) and 3-deoxyglucosone (3-DG) from

metabolic degradation of D-glucose or fragmentation of glycation intermediates. Diabetic and AD patients were both found to have increased RCS levels in their circulatory systems [12, 13]. These dicarbonyl compounds participate in glycation at a proportionally faster rate compared to D-glucose [14, 15], among which MGO is one of the most reactive glycation agents. MGO reacts with lysine and arginine residues on proteins to generate dicarbonyl-derived AGEs thereby aggravating the modification of proteins and prompting the formation of AGEs [16]. Thus, MGO is a relevant target for inhibitors which can prevent the formation of AGEs and minimize the undesired consequences of protein glycation.

The first and most well-known synthetic glycation inhibitor is aminoguanidine (AG) [17] which prevents the formation of AGEs by reacting with RCS such as MGO or Gly thus hindering the late stage of glycation. Though AG was terminated in phase III clinical trial in diabetic patients due to its side effects, inhibition of glycation by scavenging RCS has been proven to be an important mechanism to reduce glycation.

Several studies have reported that phenolic-rich plant foods have beneficial effects against the formation of AGEs [18, 19]. Notably, the pomegranate (*Punica granatum*) fruit, which is a rich source of phenolics, in particular ellagitannins, show a wide range of biological activities including antioxidant and anti-inflammatory effects [20-22]. Moreover, pomegranate fruit juice and extracts have been shown to exert neuron-protective effects by ameliorating symptoms of AD potentially caused by the abnormal accumulation of AGEs in the brain [23, 24]. In addition, recently,

pomegranate juice has been shown to exhibit potent inhibitory effects on the formation of AGEs compared to several other commonly consumed fruit juices [25]. However, data on the underlying mechanism/s of anti-glycation action of pomegranate compounds, either natural occurring in the fruit or their *in vivo* derived metabolites, is limited.

Herein, we investigated the *in vitro* anti-glycation effects of a standardized pomegranate fruit extract (PE) along with its major phenolic constituents, punicalagin (PA; the major ellagitannin found in pomegranate) and ellagic acid (EA; formed from the hydrolysis of ellagitannins both *in vitro* and *in vivo*). The structures of the compounds are shown in Figure 1. In addition, we also included minor phenolic constituent in pomegranate, namely, gallic acid (GA), which is commonly found in plant foods. Notably, when pomegranate juice and extracts are consumed by humans, among its naturally occurring constituent phenolics, only small amounts of EA (which is formed from the hydrolysis of ellagitannins *in vivo*) is found in circulation [26, 27]. More importantly, it is the colonic microbiota-derived ellagitannin metabolites, known as urolithins (3-hydroxy-benzopyranone derivatives; see Figure 1), which are widely acknowledged as the relevant *in vivo* derived metabolites present in human subjects after the consumption of pomegranate juice and extracts [26-29]. Interestingly, these urolithin metabolites have been estimated to reach physiologically relevant concentrations through enterohepatic circulation [30]. Furthermore, these urolithins have been reported to show anti-glycative and neuroprotective activities [31].

Therefore, because of these aforementioned reasons, we also included urolithin derivatives [urolithin A (UA) and urolithin B (UB)] in the current study to investigate their potential mechanism/s of anti-glycation action. The inhibitory effects of all of the test samples were evaluated on all of the stages of glycation by the BSA-fructose and G.K. peptide-ribose assays using a combination of analytical methods including intrinsic fluorescence, MALDI-TOF mass spectrometry and circular dichroism (CD). In addition, the dicarbonyl scavenging properties of the samples were also studied and their MGO-trapping activities were determined and compared with the positive control, AG, by HPLC-DAD methods.

2. Materials and Methods

2.1. Chemicals

The following chemicals were purchased from Sigma-Aldrich Chemical Co. (St. Louis, MO, USA): Bovine serum albumin (BSA) [catalog # A4503], sodium azide [catalog # S2002], D-fructose [catalog # F2543], D-ribose[catalog # R7500], methylglyoxal (MGO) [catalog # M0252], aminoguanidine hydrochloride (AG) [catalog # 396494], gallic acid (GA) [catalog # G7384], sinapic acid [catalog # 85429], 1,2-phenylenediamine (PD) [catalog # P23938] and 2,3-dimethylquinoxaline (DQ) [catalog # D184977]. HPLC-grade acetonitrile and trifluoroacetic acid (TFA) were procured from Thermo Fisher Scientific (Rockford, IL, USA). ZipTip pipette tips with C_4 resin and 0.22 µm filter unit were obtained from EMD Millipore Co. (Billerica, MA,

USA). A commercial available standardized pomegranate extract (POMELLA^{TM}) which has been previously studied in human subjects for its safety/tolerability and bioavailability [29] was provided by Verdure Sciences, (Noblesville, IN, USA). The pomegranate extract (PE) is standardized to ca. 30% of the ellagitannin, punicalagin (PA), which is the major phenolic compound present in the pomegranate fruit. Purified samples of PA, ellagic acid (EA), urolithin A (UA), and urolithin B (UB) were isolated and/or synthesized in our laboratory as previously reported [27, 32].

2.2. BSA-fructose sample preparation

Stock solutions of 50 mg/ml BSA and 200 mM D-fructose were prepared in 0.2 M phosphate buffer, pH 7.4. Control groups contained 10 mg/ml BSA and 100 mM D-fructose in the absence of the pomegranate samples. Blank solutions included either BSA alone (10 mg/ml) or D-fructose alone (100 mM) in 0.2 M phosphate buffer. In a separate experiment, the BSA-fructose samples were mixed with different amount of the test samples, resulting in final concentrations of 0.5, 1, 2, 10, 50, 100 µg/ml for PE and 0.5, 1, 2, 10, 50, 100 µM for the pure phenolic compounds including PA, GA, EA, UA and UB. D-fructose (100 mM) and BSA (10 mg/ml) were incubated with different concentrations of AG to serve as a positive control. All reaction mixtures were prepared in triplicate and incubated under sterile conditions at 37 °C for a total length of 21 days. During incubation, aliquots were drawn from the reaction mixtures on day 3, day 7, day 14 and day 21 and stored at -20 °C until analysis. Analysis of the mixtures

was performed on samples that were thawed, centrifuged and purified by ZipTip pipettes, EMD Millipore Co. (Billerica, MA, USA).

2.3. Detection of BSA-AGEs by fluorescence

Prior to analysis, 40 µl of each BSA-fructose solution was diluted 5 fold with 160 µl 0.2 M phosphate buffer, pH 7.4, and then transferred to 96-well black fluorescence reading plates. Fluorescence measurements for monitoring glycated products were then carried out with a Spectra Max M2 spectrometer (Molecular Devices, Sunnyvale, CA, USA) at excitation and emission wavelengths of 340 nm and 435 nm, respectively. The above excitation and emission values were optimal for detecting AGEs-specific fluorescence produced from the glycation of BSA with D-fructose. Percent inhibition of AGE formation was calculated using the following equation: % inhibition = [1-(fluorescence intensity of solution with inhibitor/fluorescence intensity of control solution)] x 100%.

2.4 Circular dichroism measurements

Circular dichroism (CD) analyses were performed on a Jasco J-720 spectropolarimeter (Tokyo, Japan) using quartz cuvettes with 1 mm path length. Interpretation of results was performed by the Spectra Manager software. Prior to spectral acquisition, 10 µl BSA-fructose solution of each sample was diluted with 90 µl 0.2 M phosphate buffer, pH 7.4, resulting in a final BSA concentration of 1 mg/ml. CD spectra were obtained in the far-ultraviolet region (190 - 250 nm) employing a total of 10 consecutive scans for each sample. The bandwidth in each case was adjusted to 1

nm and 0.2 M phosphate buffer was used as blank to normalize the baseline of each reading.

2.5. MALDI-TOF mass spectrometry

10 mg/ml BSA was glycated with 100 mM D-fructose in the presence of 50 µg/ml of PE, 50 mM of the pure phenolics (PA, EA, GA, UA, UB) or 50 mM AG at 37 °C for 7 days. Intact BSA samples with or without the modification of D-fructose were purified and concentrated using C_4 ZipTips. Prior to analysis, the purified protein samples (0.7 µl) were each mixed with a 50% aqueous acetonitrile solution (0.7 µl) of saturated α-cyano-4-hydroxy-cinnamic acid containing 0.05% TFA as matrix, spotted onto a stainless steel sample plate and allowed to air dry. Samples were analyzed on a Bruker Autoflex MALDI-TOF mass spectrometer with instrument settings optimized for intact protein analysis. Spectra were acquired in linear TOF mode with a 550 nano seconds delay in the m/z range from 25,000 to 75,000. Each spectrum was the sum of 5000 single laser shots randomized over multiple positions within the same spot. Data analysis was performed using FlexAnalysis and ClinProTools software (Bruker Daltonics Inc., Billerica, MA).

2.6. G.K. Peptide-ribose assay

G.K. peptide-ribose assay was performed with slight modifications from the previously published method [33]. Briefly, 40 mg/ml G.K. peptide was incubated with 100 mM ribose in 0.1 mM sodium phosphate buffer, pH 7.4 in dark at 37 °C. The pomegranate samples or positive control, AG, were added to G.K. peptide-ribose

mixtures with concentration range of 0 to 100 µg/ml for PE and 0 to 100 µM for PA, GA, EA, UA and UB. After incubation for 6 hours, the fluorescence of each sample was obtained using a Spectra Max M2 spectrometer (Molecular Devices, Sunnyvale, CA, USA) at excitation wavelength and emission wavelength of 340 nm and 420 nm, respectively.

2.7. MGO trapping capacity evaluation

5 mM MGO solution, 20 mM derivatization reagent 1,2-phenylenediamine (PD) and 5 mM internal standard agent and 2,3-dimethylquinoxaline (DQ) were freshly prepared in 0.1 M phosphate buffer, pH 7.4. MGO solution (0.25 ml) was mixed with 0.25 ml phosphate buffer serving as blank solution or 0.25 ml of 1 mM AG serving as positive control. For the sample treatments, 0.25 ml of 100 µg/ml of PE or 1 mM of the pure compounds (PA, GA, EA, UA or UB) was individually added to 0.25 ml 5 mM MGO. After incubating at 37 °C in a shaking water bath for 1 hour, samples were removed and 0.125 ml of derivatization agent PD and 0.125 ml of internal standard solution DQ were added to each mixture. The solutions were then left at room temperature for 30 mins, allowing the derivatization reaction to be completed. The amount of 2-methylquinoxaline (2-MQ), the derivative of residual MGO, was then quantified by High performance liquid chromatography (HPLC) with diode array detection (DAD). All of the HPLC-DAD analyses was performed on a Hitachi Elite LaChrom system (Pleasanton, CA, USA) consisting of an L-2130 pump, L-2200 autosampler and L-2455 Diode Array Detector (DAD), all operated by EZChrom Elite

software. The derivatives of unreacted MGO were separated on a Phenomenex Luna C18 reverse phase HPLC column (i.d., 5 µm, 4.6 mm × 250 mm). A gradient solvent system consisting of solvent A (0.1% aqueous TFA) and solvent B (methanol) were applied as follows: 0-26 min, from 23% to 80% B; 26-27 min, 80% B; 27-28 min, from 80% to 23% B; 28-34 min, 23% B at a constant flow rate of 0.8 ml/min over 30 mins. The formation of MGO derivative products was monitored at a wavelength of 220 nm. Percent decrease of MGO was calculated using the following equation: % MGO decrease = [1 - (MGO amounts in solution with tested sample/MGO amounts in control solution)] x 100%.

3. Results and Discussion

3.1. Effect of PE and purified phenolic compounds on early stage protein glycation

At the early stage of glycation, the carbonyl group of a reducing carbohydrate condenses with the free amino group on a protein or other amino containing molecule to form Amadori products. This process results in an increase of protein mass which can be detected by MALDI-TOF mass spectrometry [34]. Proteins with a greater glycation level will have a greater mass shift compared to its natural form and the number of sugar adducts can be calculated based on such a shift using the following equation: number of sugar adducts = (molar mass of glycated protein – molar mass of natural protein)/molar mass of sugar.

Figure 2 A-D shows the MALDI-TOF profiles for samples containing natural BSA (2 A), BSA glycated with D-fructose (2 B), glycated BSA incubated with AG (2 C) or PA (2 D). The mass shifts of samples treated with other potential glycation inhibitors including PE, EA, GA, UA and UB are summarized in Table I. Natural BSA had a mass shift of 66240 Da which was in agreement with the literature [34]. After the induction of glycation with D-fructose, BSA exhibited an increased mass shift of 1460 Da, which equals to 8 fructose adducts onto the protein based on the equation explained earlier. However, a noticeable reduction in such a mass shift of BSA was observed when PE and the purified phenolics were added to the glycation model reaction. Among all of the test samples, PA and EA showed the most significant inhibitory effect of early stage glycation, resulting in a substantial decrease in the number of fructose adducts from 8 sugar molecules (control solution) to 2 (PA) and 1 (EA) sugar molecules, respectively. The other test samples, including PE, UA and UB, also showed promising anti-glycation activities. Furthermore, compared to the positive control, AG, which produced glycated BSA containing 7 fructose adducts, PE, UA and UB had inhibitory effects similar or slightly higher, resulting in adducts numbers ranging from 5 to 7 molecules. Interestingly, the phenolic compound GA, which is a very minor constituent in pomegranate compared to PA and EA, but commonly present in many plant foods, did not show significant inhibitory effect against the formation of early stage glycation products, generating a MALDI spectrum similar to that of the control solution

containing BSA and D-fructose only. Therefore, PA and EA are the major contributors to the early stage anti-glycation effects of PE.

3.2. Effect of PE and purified phenolic compounds on middle stage protein glycation

In the middle stage of glycation, Amadori products generated from early glycation could, over time, undergo dehydration, cyclization, oxidation, and rearrangement to form fluorescent AGEs such as pentosidine. In this study, we co-incubated BSA and D-fructose to simulate such a process and adopted this model reaction to evaluate the inhibitory activity of different doses of the test samples on the formation of middle stage glycation products. After incubation, the intrinsic fluorescence intensity of each sample was determined at excitation and emission wavelengths optimal for detecting middle stage fluorescence AGEs. The percent inhibition was calculated based on the equation explained earlier and IC_{50} values were calculated from the dose inhibition curves using Excel software.

As shown in Figure 3 A, the inhibitory effect of PE on middle stage glycation was observed even at a low dose of 0.5 µg/ml with 6.29% inhibition. As expected, PE's inhibitory effect increased (to 87.91%) when its concentration was increased to 100 µg/ml. In comparison, at an equivalent concentration of 100 µg/ml, the positive control, AG, only inhibited glycation by 57.68%. Similarly, as shown in the dose-inhibition curves in Figure 3 B, compounds PA, GA, EA, UA and UB all showed anti-glycation activities and inhibited the formation of middle stage fluorescent AGEs by 90.74, 60.00, 70.52, 23.67 and 29.88%, respectively, when their concentration was increased

to 100 μM. Among the pure compounds, PA had the strongest inhibitory effect on middle stage glycation with an IC_{50} value of 47.32 μM while the IC_{50} of the positive control, AG, was 876.55 μM which was about 18 fold more than PA. In addition, GA and EA also showed lower IC_{50} values (81.03 μM and 58.66 μM, respectively) than that of AG, indicating that they are more potent glycation inhibitors compared to the positive control. UA and UB had similar anti-AGEs activities than that of AG, with IC_{50} values of 924.15 μM and 741.36 μM, respectively. It should be noted that AG showed similar inhibitory effects and IC_{50} values in both Figures 3 A and 3 B (see Supplementary Figure 1 which shows the anti-AGE activities of AG with unit conversion of μg/ml).

The alteration in the secondary structure of a protein is a valuable index to assess the undesired consequences of glycation modification. The secondary structure of BSA is composed of about 67% α-helix structure and its conformational change can be determined by monitoring the loss of α-helix structure using CD spectrometry. To evaluate the effect of the pomegranate samples on the conformational change of glycated protein, BSA was incubated with D-fructose in the absence or presence of the samples and the CD spectrum was taken for each sample at the far UV region. Figure 4 displays the respective CD profiles of the reaction solutions containing natural BSA, glycated BSA, or BSA-fructose mixtures treated with inhibitors.

Native BSA exhibited a CD spectrum with well-defined α-helical features. These features were comprised of two prominent dips in the UV spectrum with one occurring at 210 nm and the other at 222 nm. The BSA and D-fructose mixture, however,

showed drastic reduction of the featured helical pattern, indicating that BSA has lost α-helix structures during glycation due to the formation of AGEs and the consequent protein conformation change. More importantly, Figure 4 revealed that the pomegranate phenolics, PA and EA, protected BSA from glycation by D-fructose, producing CD spectral profiles almost superposed to that of natural BSA. Similarly, PE, GA, UA, and UB also reduced the conformational change of BSA, but were less protective of the protein's α-helical structure compared to PA and EA (see Supplementary Figure 2). The combination of intrinsic fluorescence and CD results demonstrated the protective effects of PE and the purified phenolics on middle stage glycation suggesting that these substances could help to maintain proteins' secondary structure during the glycation process.

3.1. Effect of PE and purified phenolic compounds on late stage protein glycation

Late stage AGEs such as glyoxal lysine dimer (GOLD) and methylglyoxal lysine dimer (MOLD) are responsible for protein crosslinking on longest-lived extracellular proteins. This crosslinking process has been implicated as strong contributors to many progressive diseases of aging, including vascular diseases, stiffness of joints, arthritis and kidney failure [1, 3, 35]. A model reaction containing G.K. peptide and D-ribose was adopted in this study to evaluate the inhibitory effect of different concentrations of PE and the purified phenolics on late stage glycation and the formation of crosslinking AGEs. After 6 hours of incubation, the glycation products were characterized by their intrinsic fluorescence and the intensity values are shown in Figure 5. PA inhibited late

stage glycation in a dose-response manner, producing inhibitory effects of 32.32, 65.00 and 98.76% at concentration of 10, 50, and 500 μM, respectively. EA also showed promising inhibitory effects by reducing the formation of late stage AGEs by 34.68, 45.49 and 40.91% at doses of 10, 50 and 500 μM, respectively. In comparison, AG produced similar inhibition level but at a much higher concentration of 5 mM.

3.4. Scavenging activity of pomegranate samples on RCS

Figure 6 shows the HPLC-DAD profiles of MGO derivatives obtained from MGO solutions with or without the treatment of glycation inhibitors. In the HPLC profiles, peaks 1, 2 and 3 represent unreacted derivatization agent PD (1,2-phenylenediamine), MGO derivatives 2-methylquinoxaline (2-MQ) and internal standard, 2,3-dimethylquinoxaline (DQ), respectively. The percent decrease of MGO in each sample is summarized in Table II. As expected, the MGO content decreased to 53.7% in the solution treated with 1 mM AG, a typical trapping agent of reactive carbonyl compounds. Notably, at the same concentration, PA had a much higher capability of direct MGO trapping by decreasing MGO content to 84.6%. This activity was followed by PE, which reduced MGO by 57.7% at a concentration of 50 μg/ml. GA and EA showed similar MGO scavenging activities with AG. UA and UB also showed some RCS scavenging capacities but weaker than the positive control.

In conclusion, we have shown that PE and its phenolics (naturally occurring in the fruit and their *in vivo* derived metabolites) are efficient anti-glycation agents by reducing the formation of AGEs. Among the samples, PA had the strongest inhibitory

effect at all three stages of glycation followed by PE, EA and GA. The pomegranate *in vivo* derived colonic metabolites, UA and UB, also showed anti-AGEs activity which was similar to that of positive control, AG. Moreover, PE, and the purified phenolics all exhibited MGO scavenging activity, which might be one of the possible mechanisms for their inhibitory effects on AGEs formation. The anti-glycation effects of pomegranate phenolics suggest that this food should be further investigated as a dietary approach for the prevention and/or therapy of hyperglycemia-mediated diseases such as diabetes and AD. However *in vivo* studies would be required to confirm these effects which will be pursued by our laboratory in the future.

Acknowledgments

Data were acquired from instruments located at the University of Rhode Island in the RI-INBRE core facility obtained from Grant # P20RR016457 from the National Center for Research Resources (NCRR), a component of the National Institutes of Health (NIH). HM was supported by a graduate student scholarship from the Omar Magnate Family Foundation.

References:

[1] J. DeGroot, *Curr. Opin. Pharmacol.*, 2004, **4**, 301-305.

[2] S. R. Thorpe and J. W. Baynes, *Amino Acids*, 2003, **25**, 275-281.

[3] P. Ulrich and A. Cerami, *Recent Prog. Horm. Res.*, 2000, **56**, 1-21.

[4] A. Negre-Salvayre, R. Salvayre, N. Augé, R. Pamplona and M. Portero-Otín, *Antioxid. Redox Signaling*, 2009, **11**, 3071−3109.

[5] S. Du Yan, X. Chen, J. Fu, M. Chen, H. Zhu, A. Roher, T. Slattery, L. Zhao, M. Nagashima, J. Morser, A. Migheli, P. Nawroth, D. Stern and A. M. Schmidt, *Nature*, 1996, **382**, 685–691.

[6] V. Srikanth, A. Maczurek, T. Phan, M. Steele, B. Westcott, D. Juskiw and G. Münch, *Neurobiol. Aging*, 2011, **32**, 763-777.

[7] S. C. Chen, J. Y. Guh, C. C. Hwang, S. J. Chiou, T. D. Lin, Y. M. Ko, J. S. Huang, Y. L. Yang and L. Y. Chuang, *J. Cell Biochem.*, 2010, **109**, 38-48.

[8] V. M. Monnier, D. R. Sell, R. H. Nagaraj, S. Miyata, S. Grandhee, P. Odetti and S. A. Ibrahim, *Diabetes*, 1992, **41**, 36-41.

[9] N. Sasaki, R. Fukatsu, K. Tsuzuki, Y. Hayashi, T. Yoshida, N. Fujii, T. Koike, I. Wakayama, R. Yanagihara, R. Garruto, N. Amano and Z. Makita, *Am. J. Pathol.*, 1998, **153**, 1149-55.

[10] S. Mruthinti, A. Sood, C. L. Humphrey, S. Swamy-Mruthinti and J. J. Buccafusco, *Neuroscience*, 2006, **142**, 463-473.

[11] M. Takeuchi and S. I. Yamagishi, *Curr. Pharm. Des.*, 2008, **14**, 973-978.

[12] M. Kalousova, J. Skrha and T. Zima, *Physiol. Res.*, 2002, **51**, 597-604.

[13] M. J. Picklo, T. J. Montine, V. Amarnath and M. D. Neely, *Toxicol. Appl. Pharm.*, 2002, **184**, 187-197.

[14] S. J. Cho, G. Roman, F. Yeboah and Y. Konishi, *Curr. Med. Chem.*, 2007, **14**, 1653-1671.

[15] W. Liu, M. A. Cohenford, L. Frost, C. Semeviratne, J. A. Dain, *Bioorg. Chem.*, 2013, **46**, 1-9.

[16] A. Schmitt, J. Schmitt, G. Münch and J. Gasic-Milencovic, *Anal. Biochem.*, 2005, **338**, 201-215.

[17] P. J. Thornalley, *Arch. Biochem. Biophys.*, 2003, **419**, 31−40.

[18] X. Peng, J. Ma, F. Chen and M. Wang, *Food Funct.*, 2011, **2**, 289-301.

[19] C. Wu, S. Huang, J. Lin and G. Yen, *Food Funct.*, 2011, **2**, 224-234.

[20] M. I. Gil, F. A. Tomás-Barberán, B. Hess-Pierce, D. M. Holcroft and A. A. Kader, *J. Agric. Food Chem.*, 2000, **48**, 4581–4589.

[21] L. S. Adams, N. P. Seeram, B. B. Aggarwal, Y. Takada, D. Sand and D. Heber, *J. Agric. Food Chem.*, 2006, **54**, 980-985.

[22] M. Rosenblat, T. Hayeka and M. Aviram, *Atherosclerosis*, 2006, **187**, 363-371.

[23] R. E. Hartman, A. Shah, A. M. Fagan, K. E. Schwetye, M. Parsadanian, R. N. Schulman, M. B. Finn and D. M. Holtzman, *Neurobiol. Dis.*, 2006, **24**, 506-515.

[24] L. Rojanathammanee, K. L. Puig and C. K. Combs, *J. Nutr.*, 2013, **143**, 597-605.

[25] P. G. Dorsey and P. Greenspan, *J. Med. Food*, 2014, **17**, 447-454.

[26] B. Cerdá, J. C. Espín, S. Parra, P. Martínez and F. A. Tomás-Barberán, *Eur. J. Nutr.*, 2004, **43**, 205-220.

[27] N. P. Seeram, S. M. Henning, Y. Zhang, M. Suchard, Z. Li and D. Heber, *J. Nutr.*, 2006, **136**, 2481-2485.

[28] N. P. Seeram, Y. Zhang, R. McKeever, S. M. Henning, R. P. Lee, M. A. Suchard, Z. Li, S. Chen, G. Thames, A. Zerlin, M. Nguyen, D. Wang, M. Dreher and D. Heber, J. *Med. Food*, 2008, **11**, 390-394.

[29] S. U. Mertens-Talcott, P. Jilma-Stohlawetz, J. Rios, L. Hingorani and H. Derendorf, *J. Agric. Food Chem.*, 2006, **54**, 8956-8961.

[30] J. C. Espín, M. Larrosa, M. T. García-Conesa and F. Tomás-Barberán, *J. Evid. Based Complementary Altern. Med.*, 2013, **2013**, 1-15.

[31] E. Verzelloni, C. Pellacani, D. Tagliazucchi, S. Tagliaferri, L. Calani, L. G. Costa, F. Brighenti and D. Del Rio, *Mol. Nutr. Food Res*., 2011, **55**, S35-S43.

[32] D. Jean-Gilles, L. Li, V. G. Vaidyanathan, R. King, B. Cho, D. R. Worthen, C. O. Chichester and N. P. Seeram, *Chem.-Biol. Interact.*, 2013, **205**, 90-99.

[33] R. H. Nagaraj, I. N. shipanova and F. M. Faust, *J. Biol. Chem.*, 1996, **271**, 19338-19345.

[34] A. Schmitt, J. Gasic-Milencovic and J. Schmitt, *Anal. Biochem.*, 2005, **346**, 101-106.

[35] D. R. Sell and V. M. Monnier, *J. Clin. Invest.*, 1990, **85**, 380-384.

Figure Legends:

Figure 1. Chemical structures of pomegranate phenolics and their *in vivo* colonic-microbiota derived metabolites.

Figure 2. MALDI-TOF spectral profiles for samples containing natural BSA, glycated BSA, or glycated BSA treated with glycation inhibitors incubated at 37 °C for 7 days. Aminoguanidine (AG) was used as positive control. The spectrum peak indicates the doubly charged glycated BSA (z=2).

Figure 3. Percent inhibition of different concentrations of PE (A) and purified phenolic compounds (B) on the formation of fluorescence AGEs from BSA-fructose model reactions after 21 days incubation. Each point represents the average of three separate readings.

Figure 4. CD profiles of reaction mixtures of natural BSA, glycated BSA, or glycated BSA treated with inhibitors. BSA concentration was diluted to 1 mg/ml with 0.2 M phosphate buffer before analysis. Repeat scan revealed no significant difference in the spectra.

Figure 5. G.K. peptide profiles of reactions with or without the treatment of different concentrations of anti-glycation agents. 5 mM Aminoguanidine (AG) was used as positive control. Each intensity value represents the average of three separate readings.

Figure 6. HPLC-DAD profiles of MGO derivatives obtained from MGO solutions with or without the treatment of glycation inhibitors. The control mixture consisted of 1 mM

MGO, internal standard and derivatization agent only (A). In groups B and C, 1 mM MGO solutions were treated with 50 µM punicalagin (B) or 50 µg/ml pomegranate extract (C). 50 µM Aminoguanidine served as positive control (D). Peaks 1, 2 and 3 represent unreacted derivatization agent PD, MGO derivatives 2-MQ, and internal standard DQ, respectively.

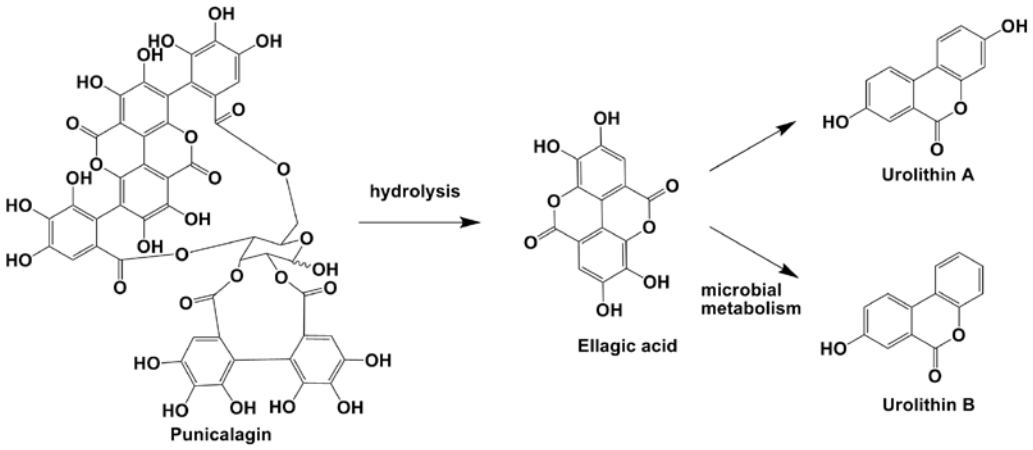

Figure 1. Chemical structures of pomegranate phenolics and their *in vivo* colonic-microbiota derived metabolites.

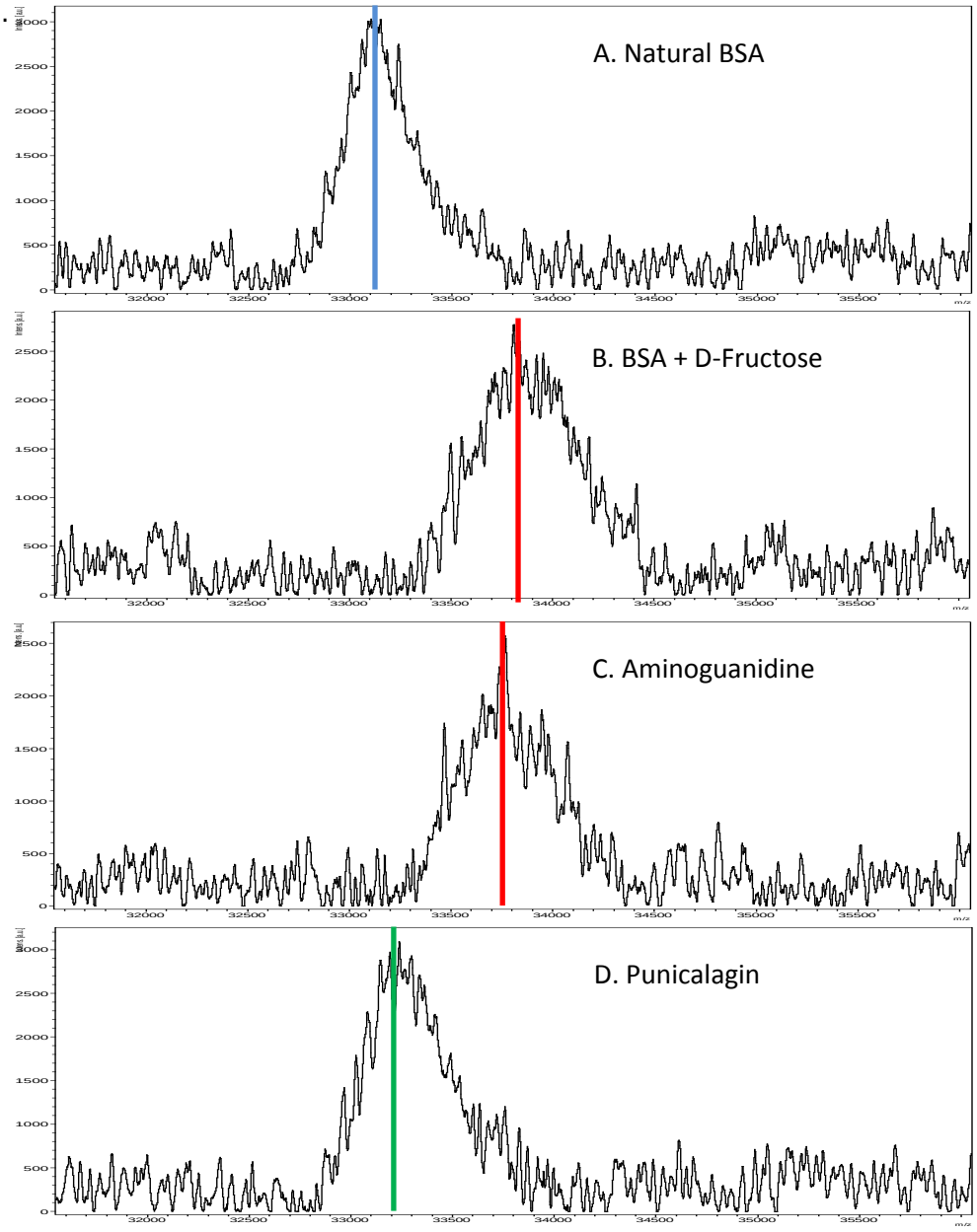

Figure 2. MALDI-TOF spectral profiles for samples containing natural BSA, glycated BSA or glycated BSA treated with glycation inhibitors incubated at 37 °C for 7 days. Aminoguanidine (AG) was used as positive control. The spectrum peak indicates the doubly charged glycated BSA (z=2).

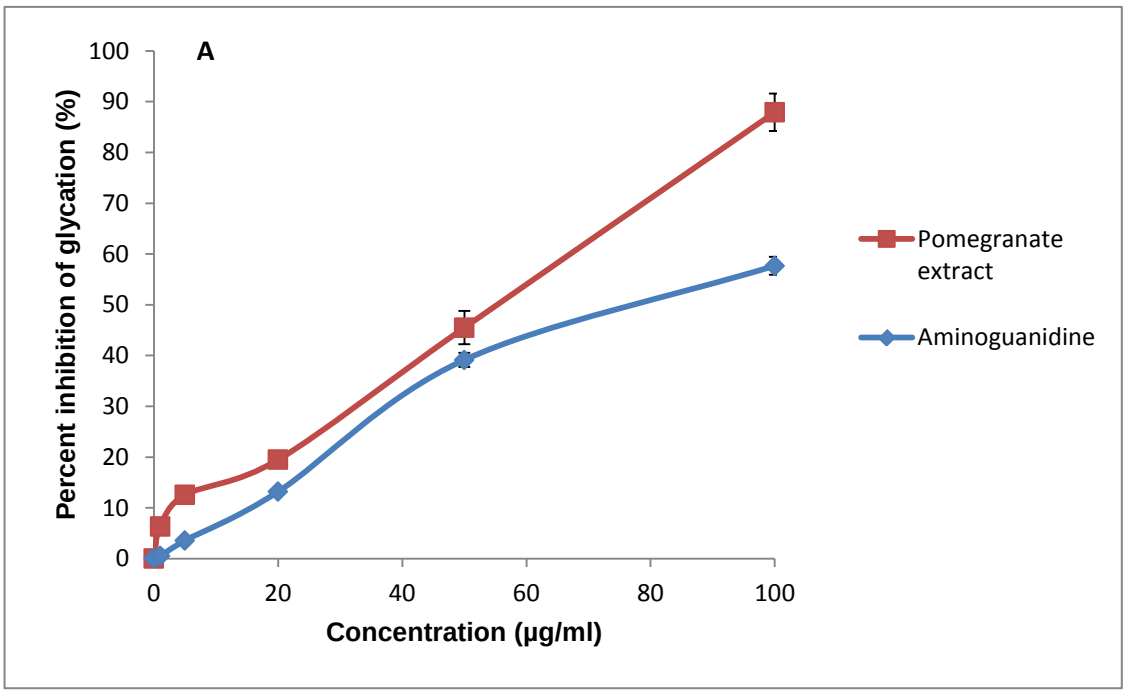

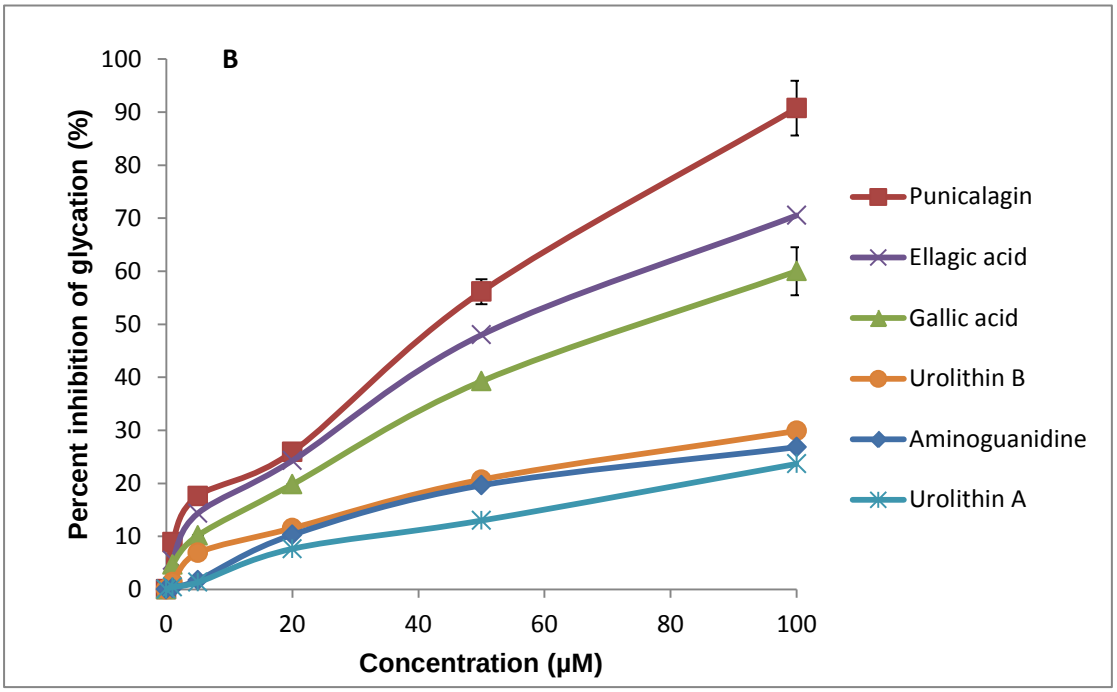

Figure 3. Percent inhibition of different concentrations of PE (A) and purified phenolic compounds (B) on the formation of fluorescence AGEs from BSA-fructose model reactions after 21 days incubation. Each point represents the average of three separate readings.

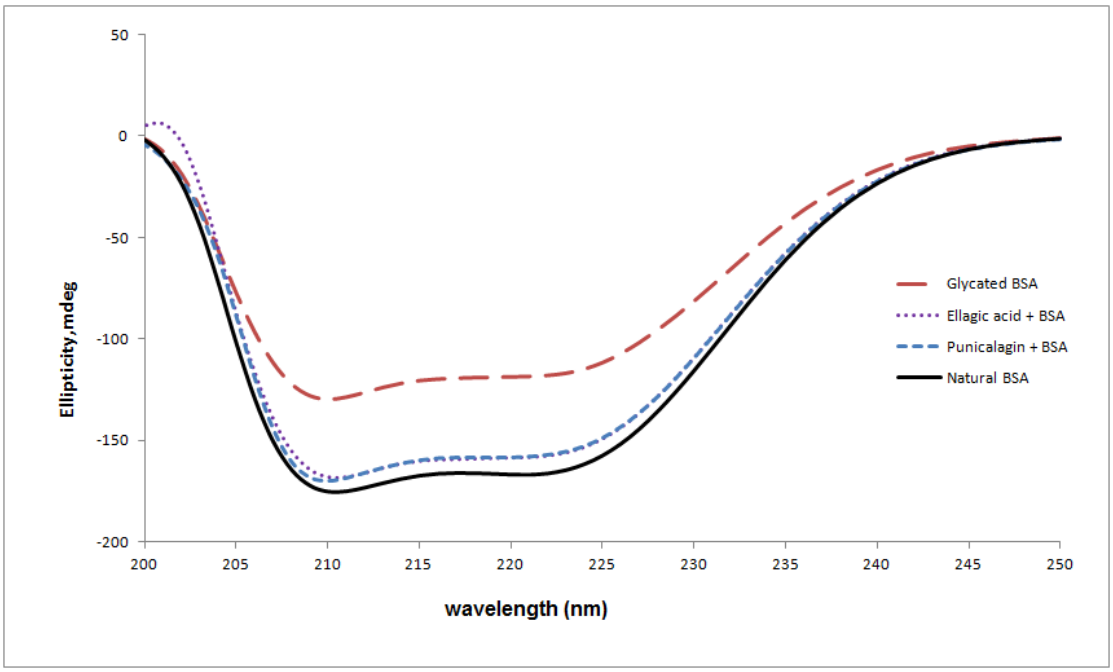

Figure 4. CD profiles of reaction mixtures of natural BSA, glycated BSA or glycated BSA treated with inhibitors. BSA concentration was diluted to 1 mg/ml with 0.2 M phosphate buffer before analysis. Repeat scan revealed no significant difference in the spectra.

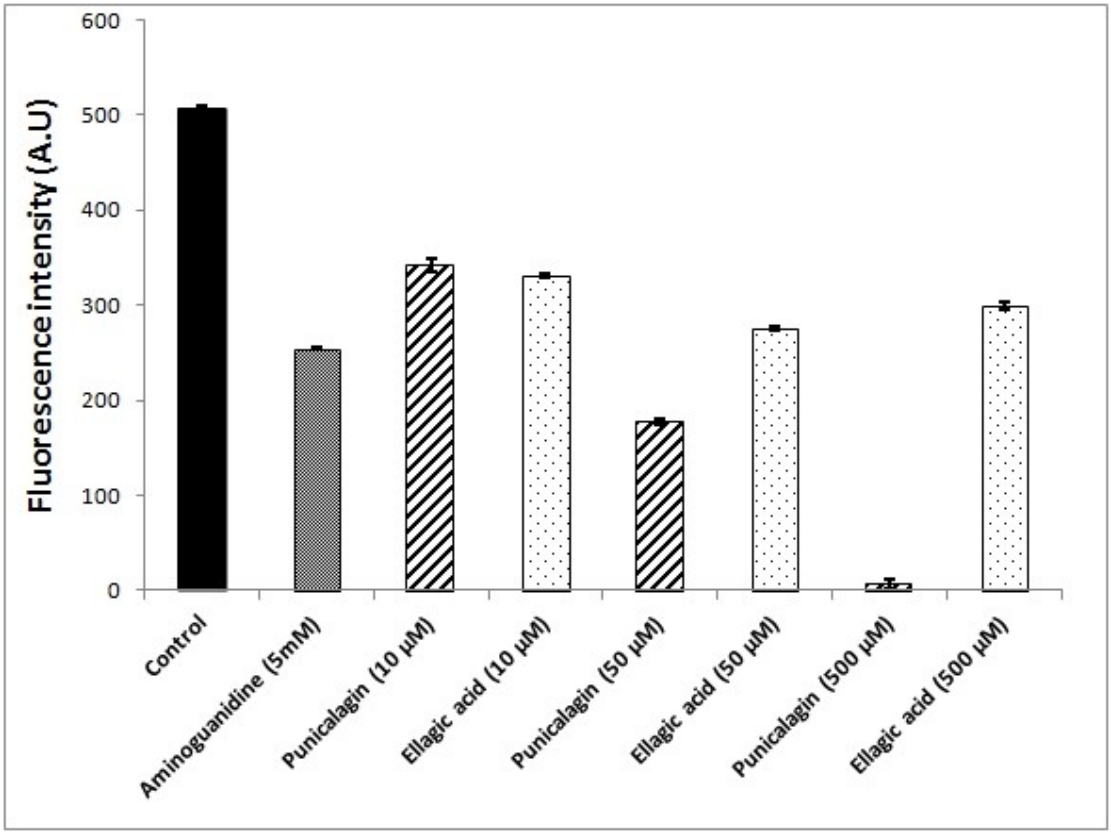

Figure 5. G.K. peptide profiles of reactions with or without the treatment of different concentrations of anti-glycation agents. 5 mM Aminoguanidine (AG) was used as positive control. Each intensity value represents the average of three separate readings.

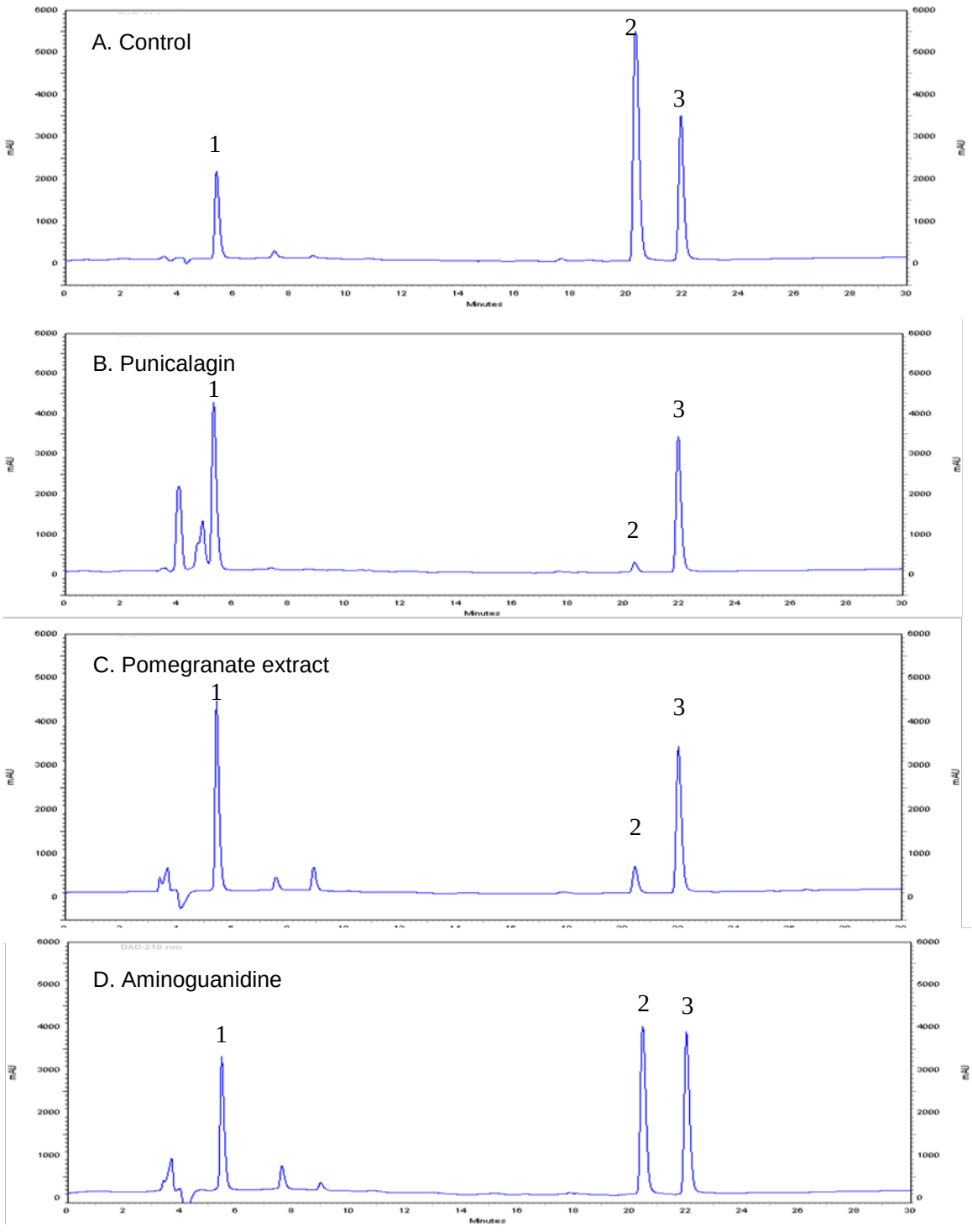

Figure 6. HPLC-DAD profiles of MGO derivatives obtained from MGO solutions with or without the treatment of glycation inhibitors. Control mixture consisted of 1 mM MGO, internal standard and derivatization agent only (A). In group B and C, 1 mM MGO solutions were treated with 50 μM punicalagin (B) or 50 μg/ml pomegranate extract

(C). 50 μM Aminoguanidine served as positive control (D). Peaks 1, 2 and 3 represent unreacted derivatization agent PD, MGO derivatives 2-MQ and internal standard DQ respectively.

Table I

MALDI-TOF analysis of m/z value and number of D-fructose adducts after glycation based on mass shifts compared to natural BSA

Sample	Mass of +2 ion	Mass of +1 Ion	Mass Shift compared to natural BSA	Number of fructose adducts
BSA	33,120 Da	66,240 Da	0	**0**
BSA + Fructose	33,850 Da	67,700 Da	+1460 Da	**8**
* **Aminoguanidine**	33,750 Da	67,500 Da	+1260 Da	**7**
Gallic Acid	33,850 Da	67,700 Da	+1460 Da	**8**
Ellagic Acid	33,230 Da	66,460 Da	+220 Da	**1**
Punicalagin	33,260 Da	66,520 Da	+280 Da	**2**
Pomegranate Extract	33,730 Da	67,460 Da	+1220 Da	**7**
Urolithin A	33,610 Da	67,220 Da	+980 Da	**5**
Urolithin B	33,690 Da	67,380 Da	+1140 Da	**6**

* 50 µM aminoguanidine was used as a positive control.

Table II

Percentage decrease in MGO after incubation with pomegranate extract (50 ppm) or phenolic compounds (50 μM) with MGO for 1 hour

Sample	HPLC peak area ratio: 2-MQ/IS	Percent MGO decrease (%)
Control	1.49	0
***Aminoguanidine**	0.69	53.7
Gallic Acid	0.86	42.3
Ellagic Acid	0.77	48.3
Punicalagin	0.23	84.6
Pomegranate Extract	0.63	57.7
Urolithin A	1.34	10.1
Urolithin B	1.27	14.8

* 50 μM aminoguanidine was used as a positive control.